# CHARACTERIZATION OF A TWO DIMENSIONAL AIR CURTAIN

*Enrico Nino, Rocco. Fasanella, Rocco Mario Di Tommaso*

A physical separation between two environments can be useful realized by means of a two dimensional gaseous jet, often called air curtain. The typical applications of this kind of devices concerned the physical separation of the adjacent environments with different pollutant levels. In particular the paper investigates the behavior of a rectangular submerged jet in rejecting dusty air from a powder zone and a clean one. The investigated jet was generated by means of a rectangular nozzle with two discharge sections respectively of 0.02x1.0 and 0.04x1.0 m ad comparing the result with previous one realized with a nozzle with section of 0.01x1.0 m. The dust has been simulated using atomized distilled water dispersed in a cloud of small droplets, sprayed transversally the air curtain. Experiments have been performed running the air curtain at Reynolds Number (*Re*) ranging from 4500 to 25500, for all the nozzle's configuration investigated. The water spray has been characterized using a Phase Döppler Particle Analyzer (PDPA), and the air curtain has been investigated by means of a Particle Image Velocimetry (PIV) technique. The amount of droplets that are able to cross the air curtain was measured, in dependence of *Re* and thickness of the air curtain.

## INTRODUCTION

As well known the air curtains constitute a separation devices adopted in order to isolate, one from each other, two adjacent air volumes with different climatic characteristics. The curtain, based on the discharge of a plane air stream, realizes a fluid insulation against heat, moisture and mass transfers between the separated areas without holding up traffic of people, vehicles, materials, objects etc.. Thus, the air curtains are particularly useful in situations where conventional physical barriers become unacceptable for practical, technical, economical or safety reasons. Applications for air curtains are many. Beside air conditioned areas, they include commercial entrances, refrigerated counters, clean rooms, testing chamber apparatus (e.g. thermal shock test chambers), industrial oven openings, tunnel fire safety systems, process line partitioning in the food or microelectronics industry, etc. [1–9].

Usually the air curtains consist of one or several jets blown vertically downwards, but upwards applications are also not so unusual. In many cases, the geometrical aspect ratio of the rectangular discharge nozzle is that of an air curtain and it may be considered as a two-dimensional plane jets. Furthermore, discharge air velocities commonly encountered in conventional devices are of the order of a few meters per second. Thus, in more academic terms, air curtains can be viewed as plane turbulent submerged jets.

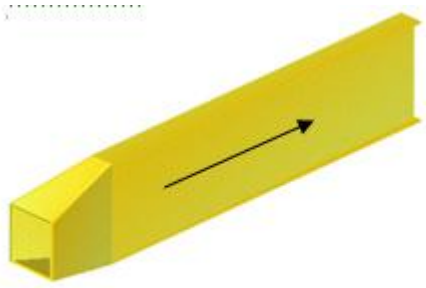

A quite large amount of study have been performed in order to infer and predict the performances of an air curtain. Several of them are based on computer simulation of the fluid dynamic of the jet (adopted in order to realize the air curtain) and the environmental surroundings. In several applications, as for instance in gates of stores workshop and cool warehouses, electronic industries and surgery units, the air curtain is used to keep high the air quality (Hayes and Stoecker [10, 11]; Partyka [12]); for the safety in underground tunnels, and in case of fire in gallery, air curtains could reduce the moving of toxic smokes while preserving full access to emergency exit, that is a obstacle to the mass transfer. Robertson and Shaw [13], indicated that these devices could reduce chemical species, odors, bacteria, dust, insects, moisture or radioactive particles transfer. Grasmuk [14] and Powlesland [15] report that air curtain's device is also applied to air stopping and flow regulation in mine airways. Guyonnaud et al [16] and Havet et al [17] investigated, also, the effect of external pressure perturbations on the performances of an air curtain adopted in order to separate two environments with different concentration of gaseous pollutant. Gupta et all. [18] investigated smoke confinements in tunnels studying the air-curtain by means of PIV measurement. Maurel e Solliec [19], have analyzed the jet development for various geometrical and cinematic configuration, using Particle Image Velocimetry (PIV) and Laser Döppler Velocimetry (LDV). Finally Nino et all. [21] performed an experiments in which a planar two dimensional submerged jet have been investigated with the porpoise of evaluate the ability of reject particulate (simulated by means of a cloud of small droplets dispersed by means of an aerosol generator). The present paper represents a sort of continuation of the activity presented in [21] with an extension represented by a change in the jet's thickness. In the previous work the authors investigated only a jet with an initial thickness of 0.01 m (equal at the nozzle height) while in the present paper the authors presents experimental results obtained with a jet's thickness of 0.02 and 0.04 m.

In the paper are reported the results obtained performing an experimental investigation on the interaction between two jets, a flat submerged jet, simulating an air barrier, and a liquid jet atomized as a spray, simulating a powder flow impacting, with a significant momentum distribution, across the air barrier in order to infer the capability of a two dimensional jet to obstacle the penetration of particles (droplets) with a density (water) much higher than the gas density (air) at a comparable velocity.

In order to infer the fluid dynamic characteristics of the air curtain and the water spray, two optical techniques have been adopted: Particle Image Velocimetry (PIV), adopted in order to measure the velocity flow field generated in the exit region of the air curtain; Phase Döppler Particle Analyzer (PDPA), adopted in order to measure velocity and diameter distribution of the droplets generate by the water spray. In particular, the measurements have been performed on the droplets cloud produced by the spray and on the droplets able to pass through the air curtain.

***Experimental Apparatus***

The flat air jet which was investigated has been obtained by directing the air flow generated by means of a centrifugal fan, equipped with electronic inverter for the regulation of the speed range, into a suited nozzle. In order to stabilize the air flow produced by the fan, the nozzle is realized by means of a convergent duct followed by a constant section duct with three different rectangular discharge section (section A, B and C) with dimensions equal respectively at h=0.01m and l=0.42 m (A); h=0.02m and l=0.42 m (B), h=0.04m and l=0.42 m (C). While the length of the constant section duct have been kept at a length as high as 1,25 m, in fig. 1 a rendering images of the investigated nozzle is reported.

The pollutant particles, interacting with the air curtain, have been simulated by means of a cloud of multi-dispersed droplets generated by means of an airbrush. In the experimental layout the airbrush axis is positioned orthogonally to the main plane of the air jet, at a distance Z=380 mm, from the air curtain central plane.

Fig. 1. Rendering of the nozzle adopted for the air curtain generation.

The capacity of the air curtain to constitute an obstacle for the liquid particles issued by the airbrush has been investigated in terms of dimensions and velocity of the survived particles beyond the curtain plane, as a function of two parameters: the distance X of the spray nozzle from the outlet section of the air curtain, which has been varied from 100 to 2000 mm.; and the air flow rate of the centrifugal fan. On the other hand, the distance Y of the Phase Döppler Particle Analyzer control volume from the spray nozzle was kept fix and equal to 420 mm. (fig. 2).

Fig. 2. Relative positioning of the spray, air curtain and measurement control volume of the PDPA.

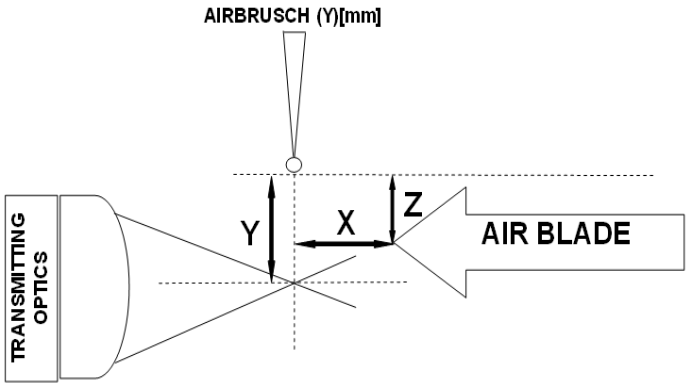


***Phase Döppler Particle Analyzer***

The determination of the statistical distributions and of the mean values of velocity vectors and diameters of liquid particles, has been obtained by means of Phase Döppler Particle Analyzer (PDPA).
The PDPA technique is a combination of a Laser Döppler Velocimetry (LDV), used to measure velocity values of seeding particles inside a flow, with another laser optic technique, which is able to obtain dimensional measures of liquid or solid particles, and based on signal phase acquisitions. The adopted PDPA layout is reported in fig. 3.

Fig. 3. PDPA layout.

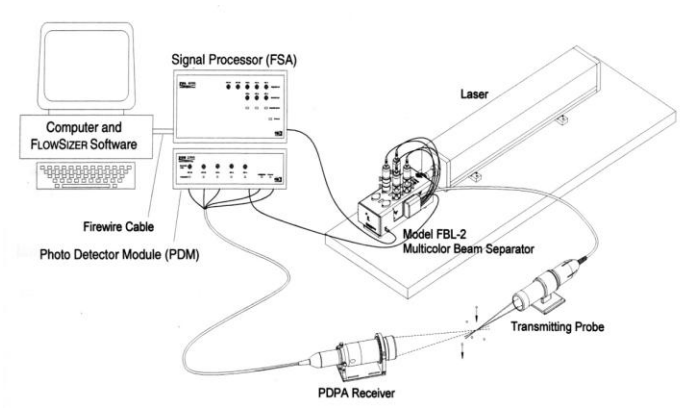

The beam, issued by a continuous laser source, is split into two or more components of equal intensity. The frontal spherical lens of the transmitting optics modifies the beam directions, initially parallel, causing the intersection in its focal point. This crossing volume represents the instrument measurement volume. The interference phenomena in the measurement volume cause a fringe pattern (luminous and dark equidistant fringes) which allows the measurements. In fact, while a particle is crossing this zone, it is illuminated by means of the luminous radiation here present (fringe pattern) and a frequency modulated luminous signal is scattered in the surrounding space. The Photo Detector Module (PDM) receives the optical signals from the fiber-optic probes and sends them, as electrical signals, to the FSA signal processor. The FSA signal processor receives these signals and extracts information such as frequency, phase, burst transit time, burst arrival time and sends these information to the host computer. The data are analyzed using the FLOWSIZERTM software running on the PC, which displays a detailed analysis. The PDM contains three photomultiplier tubes (PMT), one for each velocity or phase signal. The signal that is sent trough a high-pass filter, in order to remove pedestal component, and trough a low pass filter (in practice, a band-pass filter) in order to remove the spurious high frequency components, acting also as anti-aliasing filter. In this application the band-pass filter (as resumed in Tab 1) was set to 1-10 MHz.

Table 1. Setup of PDPA

| Instrument setup of PDPA | | | |
|---|---|---|---|
| LDV controls | | Intensity Validatio/PVC | |
| PMT Voltage | 370 V | Min. diameter limit | 3 µm |
| Burst Tr | 30 mV | Num. of diam. beam | 100 |
| Band Pass Filter | 1 - 10 MHz | Slope of upper int. | 0.200 |
| | | curve | |
| SNR | Medium | Lower to up | 0.1 |
| Downmix Freq. | 38 MHz | Upper int. | 28.00 |
| Laser Beam diam. | 2.8 mm | Lower int. | 21.00 |

After going through the band-pass filters, the signal splits into two: one goes to the burst detector and the other to the burst sampler. The burst detector is a critical part of the signal processor. Since burst signals occur randomly, it is important to identify the occurrence of the burst so that they can be processed. The burst detector discriminates between the Döppler signal and the background noise by continually monitoring the quality (SNR value) of the incoming signal and detecting the signal when it exceeds a preset value. The incoming signals are also sampled, in parallel with the burst detector, using high-speed, multi-bit converters. They sample the signals at multiple rates simultaneously. The frequency estimate, provided by the burst detector, determines which multi-bit sampler is optimum for the actual burst frequency. Once a burst gate goes off, it signals the burst processor to read samples from the sample memory and to begin processing this data. Burst processing consists of determining the frequency of a signal. In a phase Döppler system with three-phases channels, the phase difference between these, is determined using a cross-correlation technique.

***Particle Image Velocimetry***

A PIV system has been employed to analyze the instantaneous behavior of the velocity field. The adopted system (whose layout is reported in Fig. 4) is based on two pulsed Nd:YAG lasers firing on the second harmonic (green 532 nm). The beams, properly separated in time, are recombined on the same optical path by a polarized dichroic filter. Then the beams are expanded in one direction, by a combinations of spherical (negative) and cylindrical lens, to obtain a 100 mm wide and 0.3 mm thick laser sheet in the measuring region. The laser sheet is used to illuminate the airflow generated by the nozzle. A fog generator has been used to disperse water droplets seeded in the feed duct to the test nozzle.

Fig. 4. PIV layout.

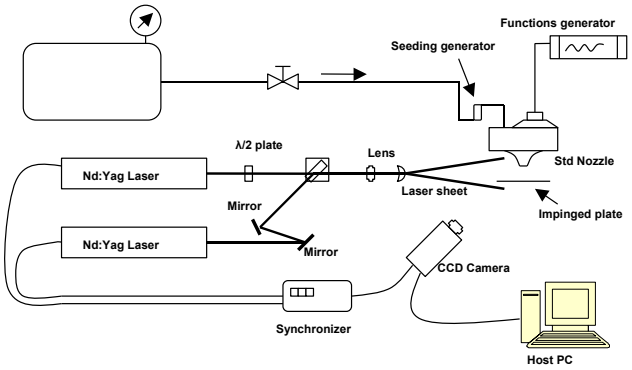


The images have been collected by of a double frame 1024 x 1024 pixels PCO CCD camera synchronized with the two laser beams and with the frame grabber by means of a dedicated electronic synchronizer. The images are formed by two different layers, each of them containing information about the seeding positions obtained by firing one of the two lasers. So the initial seeding positions (first laser beam, image on the first layer) and the final one (second laser beam, image on the second layer) are spotted.

The images were then post-processed by means of the TSI INSIGHT® V.3.2 software in order to extract the sub-images formed by 32 X 32 pixels from each layer, and to perform a cross-correlation between the two corresponding sub-images. An interrogation algorithm extracts the correlation peak position from the cross-correlation domain with a sub-pixel precision, and performs the calculation of the two velocity components for those sub-images, by a pixel-to-mm conversion factor. Interrogations are repeated, using a recursive algorithm, for the entire set of double frames images. The measured velocities are reported in a grid with size of 32 x 32 pixels with a 50% overlap (Nyquist criteria). The two laser beams have been fired at about 100 mJ per pulse (second harmonic), with separation time of 40 ms and pulse duration of 10 ns. The overall estimated error has been evaluated, according to [19 and 20], as about 4% on mean velocity.

## RESULTS AND DISCUSSIONS

### *Water Spray Characterization*

In order to simulate the powder contamination a water spray, generated by means of an airbrush, has been adopted. In this way a distribution of droplets with different velocity and diameters (i.e. different surface, volume and mass) was available. Of course solid powder, naturally or artificially present in an environment, have different characteristics than a cloud of droplets, but several motivation are at the base of the adoption of a spray instead of dispersed powder. First of all, the possibility to use a laser technique (PDPA) able to characterize, with high accuracy, dimension and velocity of the droplets. This technique works only in presence of separation surface like liquid-gas (i.e. a separation surface with a real refractive index). Solid particles, presenting an imaginary refractive index, do not allow the measure of the dimension, but only that of the velocity of the single particle, at least adopting a PDPA technique. The second motivation, less important than the previous one, is that to work with a dispersed powder requires special protections even for the operators (breath problems) and the machinery (contaminations of optics and electronics). Moreover, with a liquid spray it is easy to obtain a distribution of diameter, of the producer droplets, quite large allowing, in a single experimental measurement, investigation on the interaction between the air jet and particles (droplets) with different mass and surface (diameter). The main characteristics of the water spray (in free jet conditions) produced by the airbrush, supplied by compressed air at 2 bar, which was used to simulate pollutant particles, are reported in Fig. 5 and resumed in Table 2. Those results have been collected positioning the control volume of the PDPA device at a distance Y as high as 420 mm far away from the exit nozzle of the air brush. During this characterization the air curtain has been kept off. The results are reported in terms of an average diameter reported as D10 and D32. The diameter D10 effectively represents the mean diameter of the water particles passing in the control volume. The diameter D32 is named Mead Sauter Diameter (SMD) and is calculated dividing the volume of all the droplets passing in the control volume by the surface of all the droplets passing the control volume. The result is an indication of the volume to surface ratio, i.e. an indication of the ratio between the inertial force and the viscous force. An increase of the D32 means that the inertial force are getting preponderant than the viscous force. In our case, an increase of the D32 increases the possibility that the droplets pass the air barrier.

Fig. 6. Statistic distributions of measured velocity and diameter.

| | Flow rate 1° condition ($m^3/s$); *Re*=4500 | Flow rate 2° condition ($m^3/s$); *Re*=10000 | Flow rate 3° condition ($m^3/s$); *Re*=16500 | Flow rate 4° condition ($m^3/s$); *Re*=25500 |
|---|---|---|---|---|
| **A** Nozzle high=0.01 m | 0.027 | 0.059 | 0.098 | 0.150 |
| Mean exit velocity (m/s) | 6,40 | 14.0 | 23.3 | 35.7 |
| **B** Nozzle high=0.02 m | 0.027 | 0.059 | 0.098 | 0.150 |
| Mean exit velocity (m/s) | 3.30 | 7.00 | 11.5 | 18.0 |
| **C** Nozzle high=0.04 m | 0.027 | 0.059 | 0.098 | 0.150 |
| Mean exit velocity (m/s) | 1.70 | 3.50 | 6.80 | 9.00 |

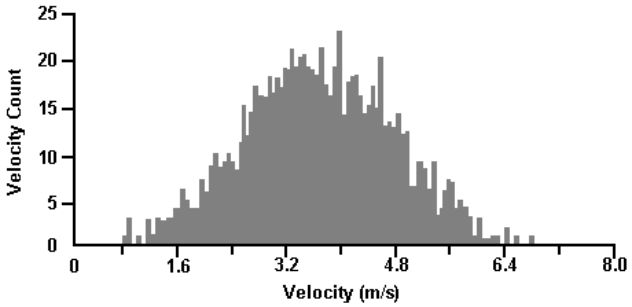


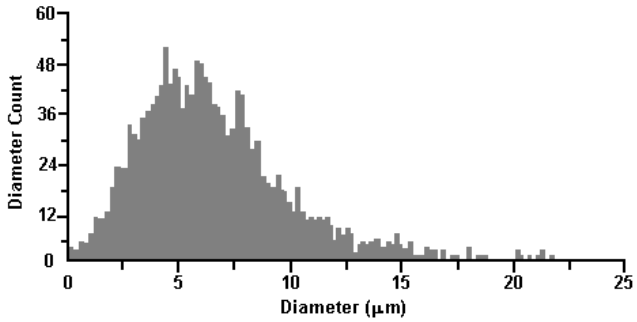


Table 2. Mean values measured on spray axis at Y=420 mm from the nozzle in absence of the air curtain.

### *Air Curtain Characterization*

The flow field generated by the air curtain have been investigated by means of a PIV technique previously described. The PIV images have been collected in a central plane positioned parallel to the nozzle axis and orthogonally to the air curtain. In particular, the air curtain have been investigated under four flow rate conditions realizing Reynolds Number (Re) equal to 4500, 10000, 16500 and 25500. The flow rates and mean exit velocity are in function of Re and nozzle configuration in Table 3.

Table 3. Experimental conditions for the three nozzles investigated.

The obtained results shows a typical situation of a submerged laminar jet, for Re ranging from 4500 to 10000, and submerged turbulent jet, for Re higher than 10000. More detail of the submerged jets investigated in the experiments are reported in [21]. A typical velocity distributions (over imposed at the PIV image) at the exit of the nozzle are reported in fig. 7 and 8 for the nozzle configuration A and Re = 4500 and Re = 16500 respectively.

Fig. 7. Velocity distribution (PIV) obtained for the submerged jet (A) at Re 4500.

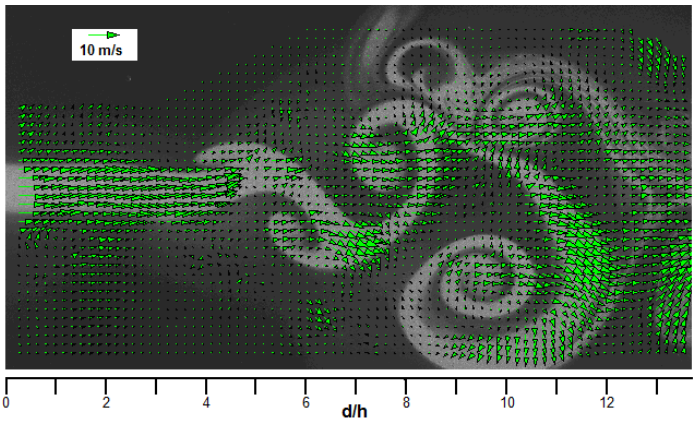


Fig. 12. Velocity distribution (PIV) obtained for the submerged jet (A) at Re 16500.

| Velocity [m/s] | D10 [µm] | Turbulence [%] | D32 [µm] |
|---|---|---|---|
| 3,5995 | 6,27 | 26,72 | 9,40 |

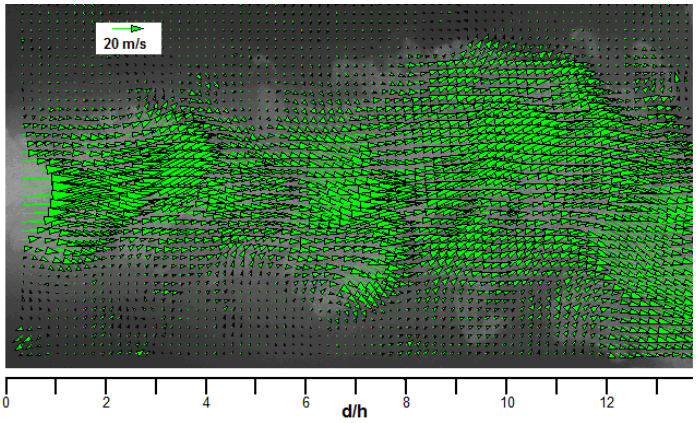


The velocity distributions obtained with the three

nozzle's configuration, under the same Re conditions are almost the same, with obvious differences in the magnitude of the velocity vectors. In particular for Re as low as 10000 the jets presents large coherent vortex while for Re as high of 14500 the jets is full turbulent with micro incoherent vortex. More details of the obtained jets are reported in [21].

***Effect of the air curtain on the spray***

For each fluid dynamic conditions and nozzle configurations the measurements have been performed keeping the air brush (adopted as spray generator) in the same position at Y = 0.42 m and moving the air curtain back and forth in dependence of the X position investigated. In that conditions PDPA have been adopted in order to measure the number, velocity and dimension of the particle sprayed by means of the air brush and able to pass the air curtain, driven at different Re conditions.
Starting with the experimental results obtained for the nozzle configuration A, discussed in [21], and reported in fig. 13 as velocity of the particles passing the curtain, in fig. 14 as the number of particles emerging from the curtain normalized by the number of particles passing in absence of curtain and fig. 15 as the diameter (D10) of the droplets. We can observe that with a moderate increase of the nozzle height, nozzle configuration B, basically all the measured parameters show a moderate decrease, in fact observing data reported in figures 16, 17 and 18 it is possible to observe how the velocity of the particles, with a distribution quite similar at what measured in the configuration A, decrease of almost 0,5 m/s (fig. 16). The same effect is visible in fig. 17 in which the normalized number of particles passing the curtain show a generalized reduction with a peak reduction at a distance, from the nozzle, of 0.5 m and a Re = 4500. Also the measured diameter show a moderate reduction (fig. 18). In the configuration C a completely different situation have been measured. In fact with a nozzle eight as high as 0.04 m and maintaining the same Re, probably the air velocity at the exit of the nozzle is too low so the air curtain generate by the nozzle C seems less able to reject the droplets. It is possible to see this effect observing, in fig. 19, the velocity of the particles generally a little bit more higher than the velocity measured with the nozzle A and B. The effect is more evident in fig. 20, in which the ration n/n0 is reported, and the number of particle passing the curtain is higher that the number measured in the other configuration, with a peak of 0.95 measured for Re = 4500, i.e. almost all the droplets sprayed pass the curtain. Also the diameter distribution of the droplets passing the curtain (fig. 21) show an average value similar at the mean value of the unperturbed spray. For the nozzle in configuration C also for a Re as high as 25500 some particles are able to pass the curtain at least in the position X = 0,1 and 0,2 m.

Fig. 13. Mean velocity versus X distance from nozzle (A) outlet section.

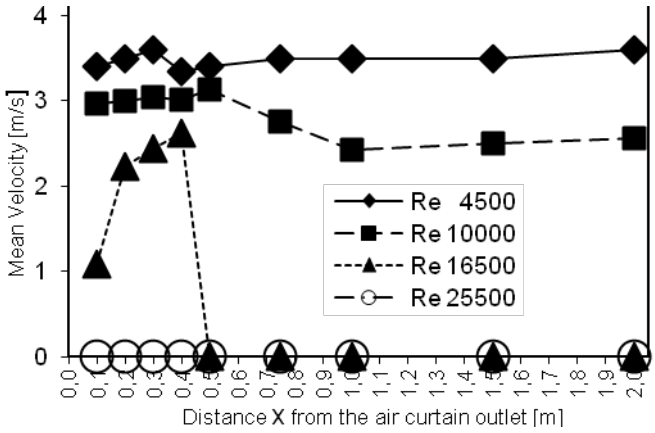

Fig. 14. Normalized particles flow rate n/n0 emerged from air curtain versus distance X from nozzle (A) outlet section.

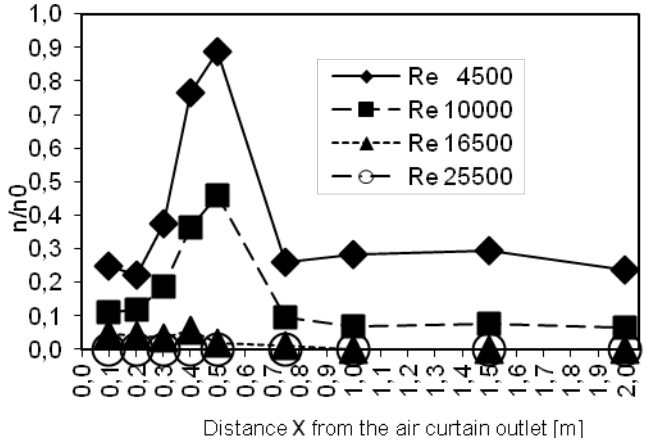


Fig.15. Mean diameters versus X distance from nozzle (A) outlet section.

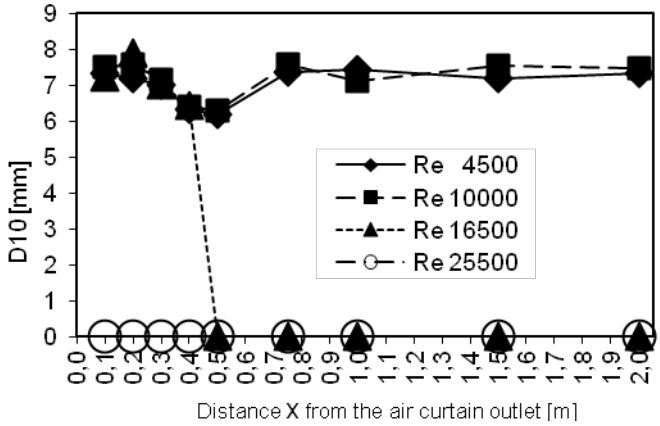


Fig. 16. Mean velocity versus X distance from nozzle (B) outlet section.

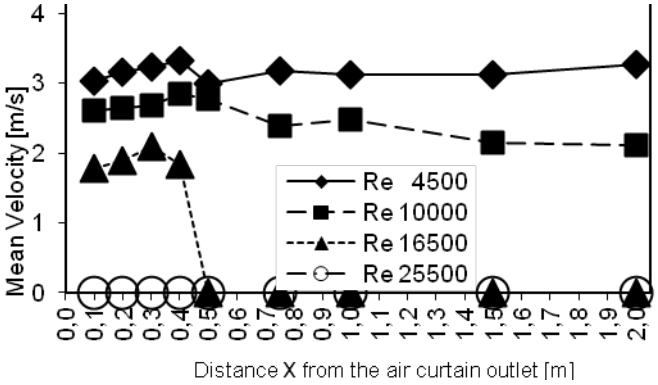


Fig. 17. Normalized particles flow rate n/n0 emerged from air curtain versus distance X from nozzle (B) outlet section.

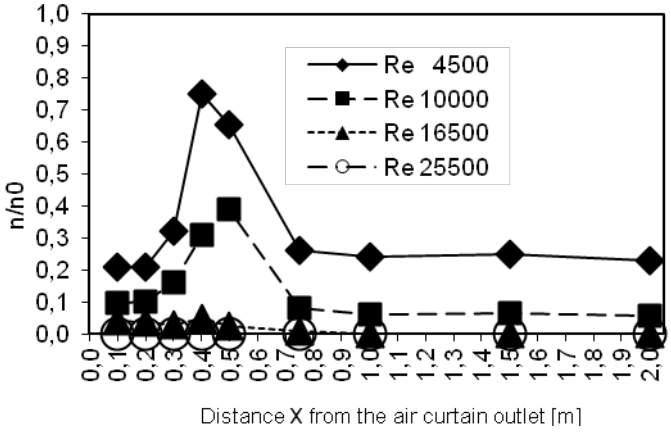


Fig. 18. Mean diameters versus X distance from nozzle (B) outlet section.

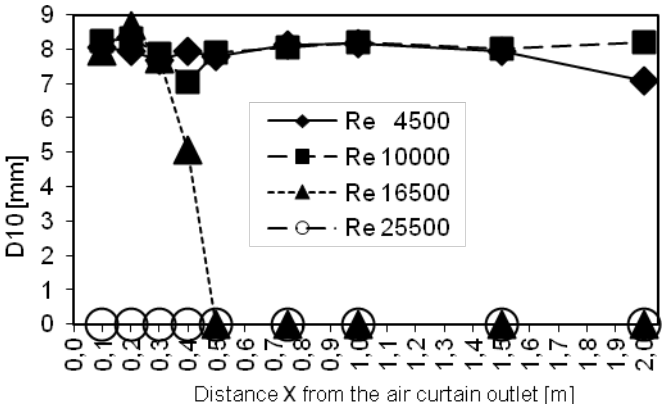

Fig. 19. Mean velocity versus X distance from nozzle (C) outlet section.

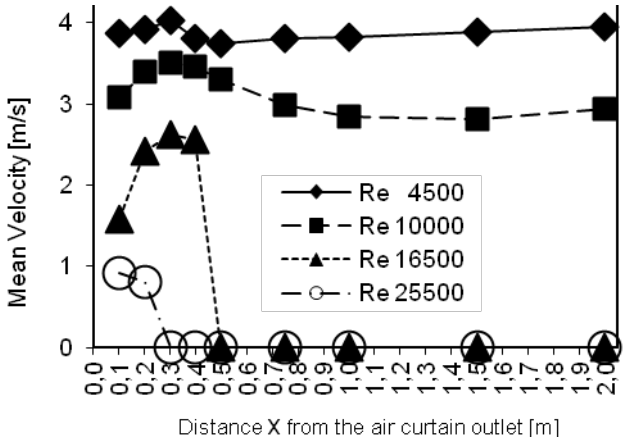


Fig. 20. Normalized particles flow rate n/n0 emerged from air curtain versus distance X from nozzle (C) outlet section.

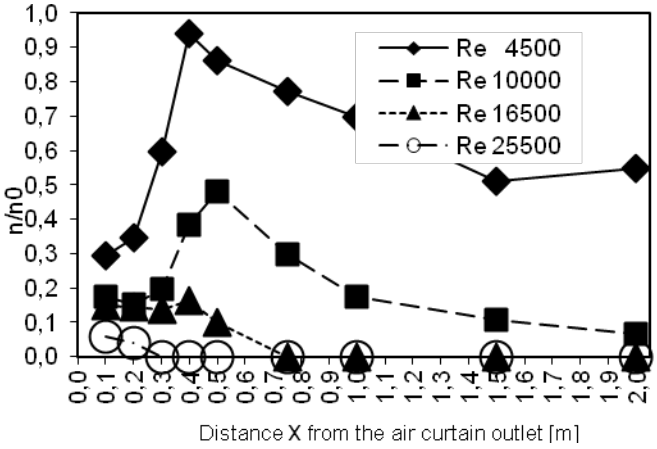


Fig. 21. Mean diameters versus X distance from nozzle (C) outlet section.

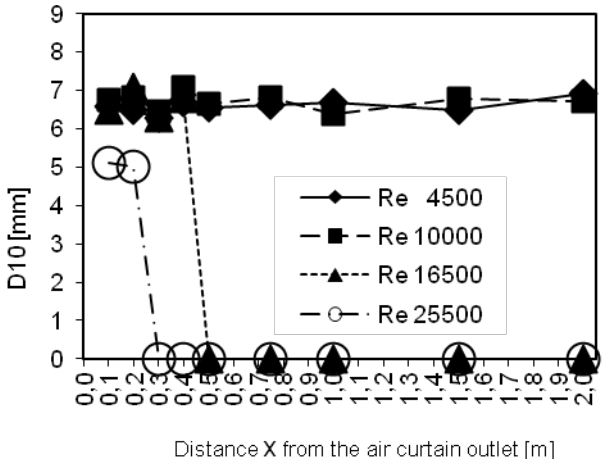


## CONCLUSIONS

In the present paper the velocity, the number and size of the droplets that are able to pass an air barrier constituted by the rectangular submerged jet, has been inferred in three nozzle configurations and in four Re conditions. The droplets cloud, simulating a dusty environment, sprayed throughout the curtain has been characterized by mean of an optical technique able to measure velocity and size distribution of the droplets forming the cloud. In particular the droplet size and sampling frequency, surviving trough the air curtain have been measured, obtaining, as main result, the dependence of the amount of droplets passing the barrier as a function of the Reynolds number of the air curtain. For a Reynolds number as high as 25500 the curtain is able to interrupt the amount of surviving droplets only for the configuration of the nozzle A and B. For the nozzle C droplets pass the curtain under all the fluid dynamic conditions investigated.

## NOMENCLATURE

| | | |
|---|---|---|
| U(x,y) | Velocity at x,y location | m/s |
| Uo | Velocity of the jet at nozzle | m/s |
| h | Exit nozzle section height | mm |
| l | Exit nozzle section width | mm |
| Uc(x) | Centerline velocity at x | m/s |

| | | |
|---|---|---|
| | location | |
| Re | Reynolds number, based on h | - |
| X | Distance between the spray nozzle and the exit nozzle exit section | mm |
| Y | Distance between the spray nozzle and PDPA measurement volume | mm |
| Z | Distance between the spray nozzle and the plane jet's board | mm |
| D10 | Droplets mean diameter | mm |
| D32 | Droplets Sauter Mean Diameter (SMD); mead droplets volume averaged by mean droplets volume | mm |

## REFERENCES

J.I. Simper, New uses for air curtains, BSE 43 (1975) A16–A18.

B. Etkin, W.D. McKinney, An air-curtain fume cabinet, Am. Ind. Hyg. Assoc. J. 53 (10) (1992) 625–631.

J. Partyka, Analytical design of an air curtain, Int. J. Model. Simul. 15 (1) (1995) 14–22.

M.A. Szatmary, Isolation chamber air curtain apparatus, Patent WO 9,850,134 (1997).

M. Pavageau, E.M. Nieto, C. Rey, Odour and VOC confining in large enclosures using air curtains, Water Sci. Technol. 44 (9) (2001) 165–171.

S.C. Hu, Y.K. Chuah, M.C. Yen, Design and evaluation of a minienvironnement for semiconductor manufacture process, Build. Environ. 37 (2002) 201–208.

P. Bridenne, P. Coffinier, Proc´ed´e et dispositif pour diffuser un flux de protection `a l'´egard d'une ambiance environnante, Patent FR 2,824,626 (2002) (Pontet et Alano SARL).

Kai Sire´n, Technical dimensioning of a vertically upwards blowing air curtain—part I. Energy and Buildings 35 (2003) 681–695

Kai Sire´n, Technical dimensioning of a vertically upwards-blowing air curtain—part II. Energy and Buildings 35 (2003) 697–705

Hayes FC; Stoecker WF Design Data for Air Curtains. Transaction of the ASHRAE n° 2121: pp 168-180. 1969 b

Hayes FC; Stoecker WF, Heat transfer characteristics of the air curtains. Transaction of the ASHRAE n° 2120: 153-167, 1969 a.

Partyka J, Analytical design of an air curtain. Int J Modelling Simulation 15: 14-22, 1995.

Roberson P; Shaw BH, The linear air curtain as a particulate barrier. J Environ Sci 21:32-33, 1978.

Grasmuk G, Applicability or air stopping and flow regulators in mine ventilation. C.I.M.M. Bullettin 62: 1175-1185, 1969.

Powlesland JW, Air curtains in controlled energy flows. Tunnels and Tunneling 52-58, 1974.

L. Guyonnaud; C. Solliec; M. Dufresne de Virel; C. Rey, Design of air curtains used for area confinement in tunnels. Experiments in Fluid 28, pp 377-384, 2000.

S. Gupta, M. Pavageau, C. Solliec, C. Rey, M. Dufresne de Virel, Particle image velocimetry measurements in air-curtain systems designed for smoke confining in the case of road tunnel fires, in: P. Strurm, S. Minarek (Eds.), Proceedings of the Second International Conference on Tunnel Safety and Ventilation, Graz, Austria, 2004, pp. 127–134.

S. Maurel, C. Solliec, A turbolent plane jet impinging nearby and far from a flat plate. Experiment in Fluids 31, pp 687-696, 2001.

M. Angioletti, R.M. Di Tommaso, E. Nino and G. Ruocco "Simultaneous Visualization of Flow Field and Evaluation of Local Heat Transfer by Transitional Impinging Jets", Int. J. Heat Mass Transfer, 46 (2003) 1703 – 1713, ISSN 0295-5075.

U. Ullum, J.J. Schmidt, P.S. Larsen, D.R. McCluskey, Statistical analysis and accuracy of PIV data, in: Proceedings of the 2nd International Symposium on PIV, Fukui, Japan, 9–11 July 1997.

E. Nino, R. Fasanella, R.M. Di Tommaso Submerged Rectangular Air Jets as a Particulate Barrier. Building and Environmental 46 (2011) 2375-2386.